02

Features of Raman scattering in lead sulfide and lead sulfide-selenide epitaxial films

© A.V. Fedorov[1], A.V. Baranov[1], S.P. Zimin[2,3]

[1] ITMO University,
197101 St. Petersburg, Russia
[2] Demidov State University,
150003 Yaroslavl, Russia
[3] Valiev Institute of Physics and Technology of RAS, Yaroslavl Branch,
150007 Yaroslavl, Russia

e-mail: zimin@uniyar.ac.ru

Received January 23, 2022
Revised January 23, 2022
Accepted February 7, 2022

Raman scattering spectra of $1-2\,\mu$m thick *n*-PbS(111) epitaxial films grown by molecular beam epitaxy on $BaF_2(111)$ substrates were obtained and analyzed. The spectra were recorded at a low excitation level of $0.36\,mW/\mu m^2$, which did not cause photo- and thermal degradation of the films. It is shown that, in accordance with the symmetry selection rules, the bands in the spectra correspond to overtone or combination tones of phonon modes of PbS at special points of the Brillouin zone. The analysis of the bands of oxides and oxysulfates of lead, which can mask the bands of lead sulfide, was carried out. The obtained data were used in the analysis of the recorded Raman scattering spectra by epitaxial films of a ternary solid solution $PbS_{0.5}Se_{0.5}$.

Keywords: Raman scattering, low excitation level, photooxidation, epitaxial films, lead sulfide, lead sulfide-selenide.

DOI: 10.21883/EOS.2022.07.54723.3193-22

Introduction

Being a narrow- and direct-gap semiconductor (0.4 eV at 300 K), lead sulfide (PbS) is used widely for the fabrication of IR emitters and detectors, gas sensors, lasers, thermoelectric elements, etc. [1–3]. The large exciton Bohr radius (18 nm) makes it possible to implement quantum dimensional effects in PbS nanoparticles of fairly large sizes [4]. The interest in fabrication of quantum dots, quantum wires, and other low-dimensional PbS objects for advanced opto- and nanoelectronic devices, thermoelectric systems, alternative energy devices, etc. [5–8], has been on the rise in recent years. It follows from the analysis of literature data (specifically, [9–15]) that Raman spectroscopy (RS), which allows one to characterize the energies of phonons in the system and relate them to the specifics of the chemical composition and the material structure, is used widely to examine bulk and nanostructured samples of lead sulfide. However, when it comes to the measurement and interpretation of bands corresponding to PbS phonons, studies often contradict each other. This is largely attributable to strong photooxidation and thermal effects induced under the influence of a laser beam in the process of measurement of Raman spectra. Photodestruction processes for lead sulfide and related chalcogenide materials PbTe and PbSe have been examined in detail by RS in [16–22]. Literature data on Raman spectra of lead sulfide suggest that, in disregard of the fact that first-order Raman scattering was predicted to be forbidden, sufficiently intense Raman bands are often associated with transverse (TO) and longitudinal (LO) phonons (see [10–12] and other studies). Theoretically, first-order Raman scattering may be allowed if the lattice symmetry is distorted as a result of doping and reduction in size to several nanometers, but the correctness of identification of these bands in each specific case requires further substantiation.

It was demonstrated in our earlier studies [22, 23] that photooxidation processes in lead chalcogenides PbTe, $Pb_{1-x}Eu_xTe$ ($x \leq 0.10$), PbSe, $Pb_{1-x}Sn_xSe$ ($x \leq 0.06$) and $Pb_{1-x}Eu_xSe$ ($x \leq 0.16$) may be minimized by lowering the excitation level. This made it possible to observe, in accordance with theoretical predictions, only overtones and combination tones of phonons at special points of the Brillouin zone in Raman spectra of epitaxial films with a high degree of structural perfection. The present study is a continuation of this research and is focused on measuring the Raman spectra of single-crystalline epitaxial PbS films under low excitation levels ($0.36\,mW/\mu m^2$) and comparing the observed bands with the results of theoretical calculations.

Experimental

The studied *n*-PbS films with a thickness of $1-2\,\mu$m were grown on $BaF_2(111)$ substrates by molecular beam epitaxy (MBE). The substrate temperature in the process of growth was 640–670 K. The similarity of lattice constants

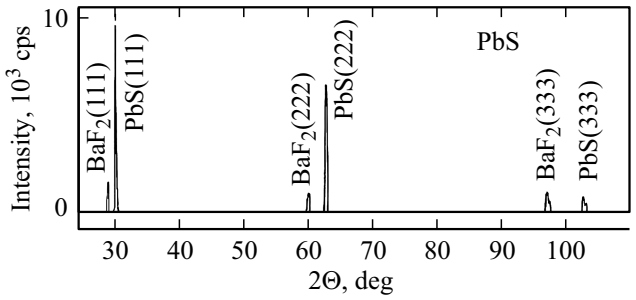

Figure 1. X-ray diffraction pattern of the PbS/BaF_2(111) epitaxial system in radiation from a cobalt source ($\lambda = 1.79$ Å).

(6.19 Å for BaF_2 and 5.94 .Å for PbS, 300 K) and thermal coefficients of linear expansion ($19.8 \cdot 10^{-6}\,K^{-1}$ for BaF_2 and $19.4 \cdot 10^{-6}\,K^{-1}$ for PbS, 300 K) of the film and the substrate established the conditions for epitaxial growth of lead sulfide layers. The results of X-ray diffraction analysis (Fig. 1) revealed that single-phase (111)-oriented PbS films had a high degree of structural perfection. A number of films were doped additionally with sodium ($\sim 1\%$); *p*-type PbS(Na) films were obtained as a result. Measurements were also performed for $PbS_{1-x}Te_x/BaF_2(111)$ films with $x = 0.03$ and $x = 0.05$ and $PbS_{1-x}Se_x/BaF_2(111)$ layers with $x = 0.5$ grown in similar MBE regimes. The $x = 0.5$ integral composition in $PbS_{1-x}Se_x$ films was determined by energy dispersive X-ray analysis. It is known [24] that $PbS_{1-x}Se_x$ solid solutions are prone to spinodal decomposition into several phases. The X-ray diffraction analysis data revealed the presence of two phases with $x = 0.51$ ($\sim 40\%$) and $x = 0.39$ ($\sim 60\%$) in the sample.

Raman spectra were measured in the backscattering geometry at room temperature with an InVia Raman microscope (Renishaw, Great Britain). An Ar^{+2} laser with an operating wavelength of 514.5 nm was used as the source of excitation radiation. The procedure of measurement of spectra was specific in that the power density of excitation radiation was minimized without sacrificing the Raman signal intensity. This was achieved using a special Renishaw Streamline^{TM} Plus system [22]. Instead of being focused into a usual spot with a diameter of $\sim 2\,\mu$m, excitation radiation with a power of 6 mW was focused in this case into a band $\sim 1 \times 50\,\mu$m in size. This helped reduce the power density of laser radiation on the sample surface by a factor of approximately 17 (to 0.36 mW/μm^2) without sacrificing the Raman signal intensity, since Streamline^{TM} allows one to utilize the entire 2D system of pixels of the CCD sensor (CCD camera) in measurement of a Raman spectrum from the entire irradiated sample surface. The signal accumulation time was 20 min at each of the three different regions of the sample; the obtained results were averaged in subsequent processing.

Identification of bands in the Raman spectrum of epitaxial PbS films with overtones and combination tones of phonons at different critical points of the Brillouin zone

Stokes shift, cm^{-1}	Data from [25,27]	Data from the present study	Presence of oxide phases
81	–	2TA(X)	+ [18,29]
95	LA(X)+TA(X) [25]	LA(X)+TA(X)	–
104	2LA(X) [25]	2LA(X) and/or 2TA(L)	–
127	TO(Δ)+TA(Δ) [25]	TO(X)+TA(X)	–
135	–	TO(X)+LA(X)	+ [17–19]
156	LA(L)+TA(L) [25] TA(Σ)+TO(Σ) [27]	LA(L)+TA(L)	–
186	–	2TO(X)	+ [17]
197	2LA(L) [25] 2TO(Δ) and/or 2TO(Σ) [27]	2LA(L)	–

Results and discussion

Figure 2 shows the Raman spectra for epitaxial film structures based on lead sulfide. A set of eight bands at 81, 95, 104, 127, 135, 156, 186, and 197 cm^{-1} has been observed for the first time experimentally for PbS films in the 60–250 cm^{-1} range. It follows from the analysis of literature sources that one or two bands are usually reported in this interval; the largest set of five bands (60, 80, 96, 156, 205 cm^{-1}) was characterized by Yin et al. [14], and four bands (78, 126,136, 180 cm^{-1}) were observed by Abu-Hariri et al. [9]. It is worth noting that the numerical values of bands in [9,14] differ; however, taken together, they match the set of values from our experiment.

When analyzing the obtained experimental results, one should take into account both the theoretically predicted bands of lead sulfide [25–28] and the known experimental bands of lead oxides and oxysulfates. The results of examination of the measured spectra are presented in the

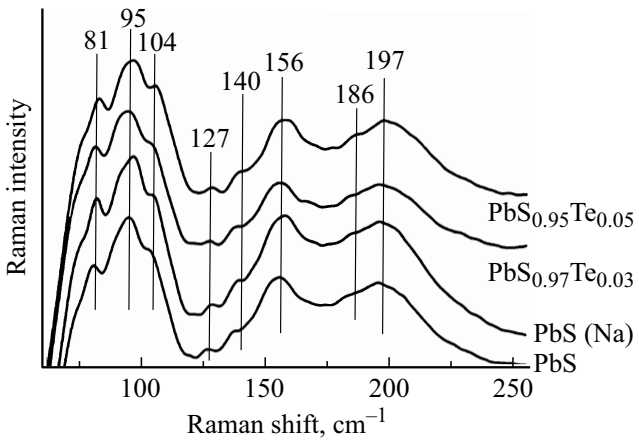

Figure 2. Raman spectra of PbS-based film structures.

table. It lists theoretical data from the most important studies [25,27], our predictions made by analyzing the phonon dispersion curves of PbS along the principal directions in the Brillouin zone [28], and data regarding the presence of oxide phases in the region. It follows from this table that the experimental set of eight bands corresponds completely to overtones and combination tones of phonons at different critical points of the Brillouin zone. At the same time, a number of bands may overlap with bands from lead oxide and oxysulfate phases, which may even produce a dominant contribution in certain cases. For example, it was found that the $81\,\mathrm{cm}^{-1}$ band is present in the spectra of all lead chalcogenides examined earlier (PbTe, PbSe, and ternary solid solutions based on them) [22,23]. This suggests that the $81\,\mathrm{cm}^{-1}$ band is related in its nature primarily to lead oxide phases, which may both be present on the initial surface and emerge in the course of photooxidation reactions under the influence of a laser beam. It follows from the analysis of literature data that the $135-140\,\mathrm{cm}^{-1}$ band is very sensitive to photooxidation processes and may be used to characterize them. Getting back to the already mentioned differences between Raman spectra in [9,14], we may conclude that the reduction in power density of excitation radiation in the experiment performed by Yin et al. [14] translated into a suppression of photo- and thermodegradation effects in the sample and provided an opportunity to measure the actual Raman spectra of lead sulfide.

Figure 2 also shows the Raman spectra for films of lead sulfide with an acceptor sodium impurity and for films of the $PbS_{1-x}Te_x$ solid solution with $x = 0.03$ and $x = 0.05$. It can be seen that, first, no bands emerge or disappear (compared to films of pure lead sulfide) in the Raman spectra measured after the introduction of sodium and substitution of a small fraction of sulfur with tellurium. Second, fine reproducibility of spectra in repeated studies of both the same sample and different samples with slightly varying compositions is indicative of the validity of the experimental procedure for Raman spectra measurement under low excitation levels.

Combined with the results for PbTe and PbSe presented in [22,23], the tabulated data for PbS allow one to analyze Raman spectra and characterize the pattern of phonon modes for the entire class of binary lead chalcogenides PbX (X = S, Se, Te). It must be understood that certain PbX bands may be masked by fairly intense bands of oxide phases produced in photooxidation processes under the influence of excitation laser radiation. Importantly, a combined set of data on the specifics of Raman spectra for binary PbX compounds allows one to proceed to the analysis of Raman spectra for ternary solid solutions based on PbX ($PbS_{1-x}Te_x$, $PbS_{1-x}Se_x$, $PbSe_{1-x}Te_x$, etc.). Let us consider a specific example of epitaxial films of the $PbS_{0.5}Se_{0.5}$ solid solution.

Figure 3 presents the Raman spectrum of the $PbS_{0.5}Se_{0.5}/BaF_2(111)$ system. This spectrum is specific in

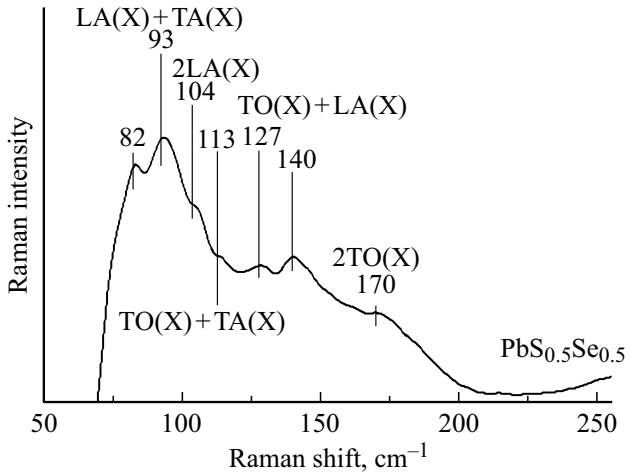

Figure 3. Raman spectrum of film $PbS_{0.5}Se_{0.5}$.

that a new wide band at $\sim 170\,\mathrm{cm}^{-1}$, which is uncharacteristic of lead sulfide (see the table) and lead selenide [22,25], emerges in it. The presence of the $176\,\mathrm{cm}^{-1}$ band has also been noted by Shao et al. [30] in the study of nanostructures of $PbS_{1-x}Se_x$ solid solutions with x varying within the 0.4–0.6 range. It is important to keep in mind that although the sets of bands for lead sulfide and selenide are close in frequencies to each other, they are interpreted with different vibrational phonon modes [25]. Therefore, the bands of PbS and PbSe of the same nature had to be compared in the analysis of the $PbS_{0.5}Se_{0.5}$ ternary solution. It is known that the 2TO(X) band corresponds to $140\,\mathrm{cm}^{-1}$ for PbSe [22,25] and $186\,\mathrm{cm}^{-1}$ for PbS (see the table). Assuming that the studied $PbS_{0.5}Se_{0.5}$ sample is a single-mode mixed crystal [31], we find that the 2TO(X) band should be located between these two values ($\sim 163\,\mathrm{cm}^{-1}$). As was already noted, the experimental samples are specific in that they feature two close phases with $x = 0.51$ ($\sim 40\%$) and $x = 0.39$ ($\sim 60\%$). In the context of interpretation of Raman spectra, this results in broadening of the 2TO(X) band and its shift from the expected frequency of $163\,\mathrm{cm}^{-1}$ toward the values typical of lead sulfide ($170\,\mathrm{cm}^{-1}$). According to [22,25], the TO(X)+LA(X) band corresponds to $120-122\,\mathrm{cm}^{-1}$ for PbSe; our data demonstrate that it corresponds to $135\,\mathrm{cm}^{-1}$ for lead sulfide. The experimentally observed broad band at $127\,\mathrm{cm}^{-1}$ for $PbS_{0.5}Se_{0.5}$ (Fig. 3) may then be attributed to TO(X)+LA(X) vibrations. The $113\,\mathrm{cm}^{-1}$ band for the ternary solid solution is likely to be associated with TO(X)+TA(X) vibrations, since the frequencies of these vibrations in lead selenide [22] and lead sulfide (see the table) are 106 and $127\,\mathrm{cm}^{-1}$, respectively. The band corresponding to 2LA(X) vibrations is at $91\,\mathrm{cm}^{-1}$ [22] and $110\,\mathrm{cm}^{-1}$ [25] for PbSe and PbS; therefore, the $104\,\mathrm{cm}^{-1}$ band for $PbS_{0.5}Se_{0.5}$ may be attributed to 2LA(X). In our view, the $93\,\mathrm{cm}^{-1}$ band for $PbS_{0.5}Se_{0.5}$ is associated with LA(X)+TA(X) vibrations, since similar vibrations for lead selenide and lead sulfide are present at $82\,\mathrm{cm}^{-1}$ [22]

and $95\,cm^{-1}$ [25], respectively. As was noted above and in [22], the remaining bands at 82 and $140\,cm^{-1}$ are probably related to photooxidation processes. These estimates suggest that, according to the existing classification [31], the studied epitaxial $PbS_{0.5}Se_{0.5}$ films belong to the group of single-mode mixed crystalline materials (with allowance for the processes of spinodal decomposition).

Conclusion

This study is the last in a series of papers focused on the examination of Raman spectra for epitaxial films of lead chalcogenides PbX (X = S, Se, Te) under low excitation levels. The applied approach, which suppresses considerably the photodegradation phenomena in the region under analysis, allowed us to characterize experimentally for the first time a wide set of Raman bands for PbTe, PbSe, and PbS with frequencies matching the frequencies of overtones and combination tones of material phonons at different critical points of the Brillouin zone. This was made possible by the use of single-crystalline epitaxial films of the studied materials with a high degree of structural perfection. The use of other objects (e.g., polycrystalline films) would result in partial distortion of spectra due to the presence of oxide phases at the grain boundaries. It is important to note that Raman spectra measurements under low excitation levels do not exclude photooxidation reactions entirely; partial oxidation of the near-surface sample layer prior to the experiment is also a possibility. Therefore, the probable bands of oxide phases, which have similar frequencies and may mask the characteristic PbX bands, should be taken into account additionally in the process of identification of bands of overtones and combination tones of PbX phonons.

Funding

This study was performed under the state assignment to the Valiev Institute of Physics and Technology of the Russian Academy of Sciences from the Ministry of Education and Science of the Russian Federation, project No. FFNN-2022-0017, and as part of the initiative research effort of the Demidov Yaroslavl State University. The authors wish to thank S.V. Vasil'ev and V.V. Osokin for providing the results of analysis of spinodal decomposition of $PbS_{1-x}Se_x$ films performed at the „Diagnostics of Micro- and Nanostructures" common use center with financial support from the Ministry of Education and Science of the Russian Federation.

Conflict of interest

The authors declare that they have no conflict of interest.

References

[1] Yu.I. Ravich, B.A. Efimova, I.A. Smirnov. *Metody issledovaniya poluprovodnikov v primenenii k khal'kogenidam svintsa PbTe, PbSe, PbS* (Nauka, Moscow, 1968) (in Russian).
[2] T.Fu. Sensors. Actuators B: Chemical, **140** (1), 116 (2009). DOI: 10.1016/j.snb.2009.03.075
[3] S. Kumar, Z.H. Khan, M.A. Majeed, K.M. Husain. Curr. Appl. Phys., **5**, 561 (2005). DOI: 10.1016/j.snb.2009.03.075
[4] F.W. Wise. Acc. Chem. Res., **33**, 773 (2000). DOI: 10.1021/ar970220q
[5] S.P. Zimin, E.S. Gorlachev. *Nanostrukturirovannye khal'kogenidy svintsa* (Izd. Yarosl. Gos. Univ., Yaroslavl, 2011) (in Russian).
[6] N. Sukharevska, D. Bederak, V.M. Goossens, J. Momand, H. Duim, D.N. Dirin, M.V. Kovalenko, B.J. Kooi, M.A. Loi. ACS Appl. Mater. Interfaces, **13**, 5195 (2021). DOI: 10.1021/acsami.0c18204
[7] T. Blachowicz, A. Ehrmann. Appl. Sci., **10**, 1743 (2020). DOI: 10.3390/app10051743
[8] X. Zhang, Y. Chen, L. Lian, Z. Zhang, Y. Liu, L. Song, C. Geng, J. Zhang, S. Xu. Nano Res., **14** (3), 628 (2021). DOI: 10.1007/s12274-020-3081-5
[9] A. Abu-Hariri, A.K. Budniak, F. Horani, E. Lifshitz. RSC Adv., **11**, 30560 (2021). DOI: 10.1039/d1ra04402h
[10] H. Cao, G. Wang, S. Zhang, X. Zhang. Nanotechnology, **17**, 3280 (2006). DOI: 10.1088/0957-4484/17/13/034
[11] J.-H. Chen, C.-G. Chao, J.-C. Ou, T.-F. Liu. Surface Science, **601**, 5142 (2007). DOI: 10.1016/j.susc.2007.04.228
[12] J.-P. Ge, J. Wang, H.-X. Zhang, X. Wang, Q. Peng, Y.-D. Li. Chem. Eur. J., **11**, 1889 (2005). DOI: 10.1002/chem.200400633
[13] G.D. Smith, S. Firth, R.J.H. Clark, M. Cardona. J. Appl. Phys., **92**, 4375 (2002). DOI: 10.1063/1.1505670
[14] P. Yin, R. Zhang, Y. Zhang, L. Guo. International J. Modern Physics B., **24** (15), 3257 (2010). DOI: 10.1142/S0217979210066422
[15] A.V. Baranov, K.V. Bogdanov, E.V. Ushakova, S.A. Cherevkov, A.V. Fedorov, S. Tscharntke. Opt. Spectrosc., **109** (2), 268 (2010). DOI: 10.1134/S0030400X10080199.
[16] Z. Peng, Y. Jiang, Y. Song, C. Wang, H. Zhang. Chem. Mater., **20** (9), 3153 (2008). DOI: 10.1021/cm703707v
[17] J.G. Shapter, M.H. Brooker, W.M. Skinner. International J. Mineral Processing, **60**, 199 (2000). DOI: 10.1016/S0301-7516(00)00017-X
[18] G. Giudici, P. Ricci, P. Lattanzi, A. Anedda. American Mineralogist, **92**, 518 (2007). DOI: 10.2138/am.2007.2181
[19] K. Stadelmann, A. Elizabeth, N.M. Sabanés, K.F. Domke. Vibrational Spectroscopy, **91**, 157 (2016). DOI: 10.1016/j.vibspec.2016.08.008
[20] S.P. Zimin, E.S. Gorlachev, N.V. Gladysheva, V.V. Naumov, V.F. Gremenok, H.G. Seidi. Opt. Spectrosc., **115** (1), 679 (2013). DOI: 10.1134/S0030400X1311026X.
[21] Y. Batonneau, C. Brémard, J. Laureyns, J.C. Merlin. J. Raman Spectroscopy, **31** (12), 1113 (2000). DOI: 10.1002/1097-4555(200012)31:12¡1113::aid-jrs653¿3.0.co;2-e
[22] M.O. Kuzivanov, S.P. Zimin, A.V. Fedorov, A.V. Baranov. Opt. Spectrosc., **119** (6), 938 (2015). DOI: 10.1134/S0030400X15120140.

[23] S.P. Zimin, E.S. Gorlachev, A.V. Baranov, S.A. Cherevkov, E. Abramof, P.H.O. Rappl. Opt. Spectrosc., **117** (5), 748 (2014). DOI: 10.1134/S0030400X14110241.
[24] M. Labidi, H. Meradji, S. Ghemid., S. Labidi, F. El Haj Hassan. Modern Physics Letters, **25** (7), 473 (2011). DOI: 10.1142/S0217984911025729
[25] K.S. Upadhyaya, M. Yadav, G.K. Upadhyaya. Phys. Stat. Sol. B, **229**, 1129 (2002). DOI: 10.1002/1521-3951(200202)229:3¡1129::AID-PSSB1129¿3.0.CO;2-6
[26] T.D. Krauss, F.W. Wise. Phys. Rev. B, **55**, 9860 (1977). DOI: 10.1103/PhysRevB.55.9860
[27] P.G. Etchegoin, M. Cardona, R. Lauck, R.J.H. Clark, J. Serrano, A.H. Romero. Phys. Stat. Sol. B, **245** (6), 1125 (2008). DOI: 10.1002/pssb.200743364
[28] O. Kilian, G. Allan, L. Wirtz. Phys. Rev. B, **80**, 245208 (2009). DOI: 10.1103/PhysRevB.80.245208
[29] O. Semeniuk, A. Csik, S. Kökényesi, A. Reznik. J. Mater. Sci., **52** (13), 7937 (2017). DOI: 10.1007/s10853-017-0998-5
[30] G. Shao, G. Chen, J. Zuo, M. Gong, Q. Yang. Langmuir, **30**, 7811 (2014). DOI: 10.1021/la501267f.1
[31] G.R. Wilkinson. Raman spectra of ionic, covalent, and metallic crystals. In: *The Raman effect, V. 2: Applications*, ed. A. Anderson. Chapter 5. (Marcel Dekker, New York, 1973).